



HAL
open science

Cellulose phosphorylation comparison and analysis of phosphate position on cellulose fibers

Fleur Rol, Cécile Sillard, Michel Bardet, Jayasubba Reddy Yarava, Lyndon Emsley, Corinne Gablin, Didier Léonard, Naceur Belgacem, Julien Bras

► **To cite this version:**

Fleur Rol, Cécile Sillard, Michel Bardet, Jayasubba Reddy Yarava, Lyndon Emsley, et al.. Cellulose phosphorylation comparison and analysis of phosphate position on cellulose fibers. Carbohydrate Polymers, 2020, 229, pp.115294. 10.1016/j.carbpol.2019.115294 . hal-02437118

HAL Id: hal-02437118

<https://hal.science/hal-02437118>

Submitted on 20 Jul 2022

HAL is a multi-disciplinary open access archive for the deposit and dissemination of scientific research documents, whether they are published or not. The documents may come from teaching and research institutions in France or abroad, or from public or private research centers.

L'archive ouverte pluridisciplinaire **HAL**, est destinée au dépôt et à la diffusion de documents scientifiques de niveau recherche, publiés ou non, émanant des établissements d'enseignement et de recherche français ou étrangers, des laboratoires publics ou privés.



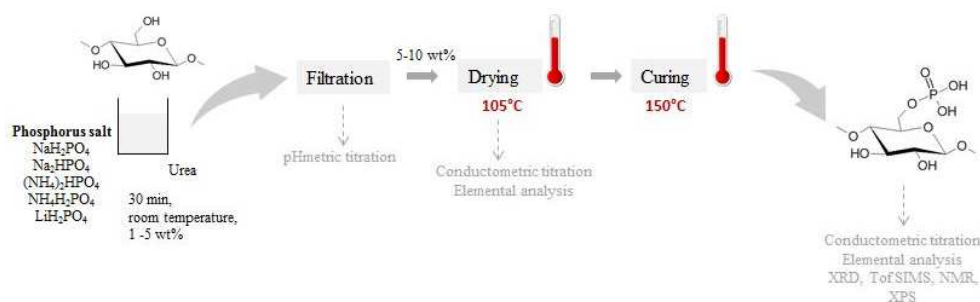
Distributed under a Creative Commons Attribution - NonCommercial 4.0 International License

31 **Keywords:** phosphorylation, cellulose, NMR, ToF-SIMS

32 **Highlights**

- 33 - Cellulose phosphorylation was studied in order to improve the final charge content
- 34 - The effect of phosphate salt constant of solubility was studied
- 35 - The position and penetration of the phosphate groups on the fibers were evaluated

36 **Abstract.** Chemical modifications of cellulose fibers as pretreatment for cellulose nanofibrils
37 (CNF) production have been investigated to improve the production process and the quality of
38 obtained cellulosic nanomaterial. In this study, phosphorylation of cellulose fibers was
39 optimized in anticipation of a future nanofibrillation. Different phosphate salts, namely
40 $\text{NH}_4\text{H}_2\text{PO}_4$, $(\text{NH}_4)_2\text{HPO}_4$, Na_2HPO_4 , NaH_2PO_4 and LiH_2PO_4 with different constants of
41 solubility (Ks) were used to increase the efficiency of the modification. Phosphorylated
42 cellulose pulps were analyzed using elemental analysis, solid-state ^{13}C and ^{31}P NMR, or
43 conductimetric titration method. No effect of Ks was observed whereas a counterion effect
44 was pointed out. The study also reported the effect of pH, cellulose concentration,
45 temperature and urea content in phosphorylation efficiency. Finally, chemical
46 functionalization and penetration of phosphorus in the cellulose fibers were evaluated using
47 XPS, SEM-EDX, ToF-SIMS and solid-state NMR.



1. Introduction

Cellulose, the most abundant polymer on Earth, can be nanofibrillated since 1980. Cellulose nanofibrils (CNF) are described in many books and reviews (Dufresne, 2013; Klemm et al., 2011; Lavoine, Desloges, Dufresne, & Bras, 2012; Rol, Belgacem, Gandini, & Bras, 2018). They are sustainable, biodegradable and biocompatible materials. CNF films are transparent, barrier and with high mechanical properties which make them useful in many applications such as packaging (Lavoine et al., 2012; Saini, Yücel Falco, Belgacem, & Bras, 2016), paper (Patent No. WO 2014118466 (A1), 2014; Brodin, 2014) or nanocomposites. However, the use of CNF is still limited due to the high energy consumption during the production. To overcome this issue, chemical pretreatments of cellulose fibers are used since 2000's to weaken the hydrogen bonds between fibers, and make the nanofibrillation easier. Moreover, CNF produced via a chemical pretreatment usually present better homogeneity and/or new functionalities as recently reviewed (Rol et al., 2018). TEMPO (2,2,6,6-Tetramethylpiperidine 1-oxyl) oxidized CNF (Isogai, Saito, & Fukuzumi, 2011) are classically produced and present higher quality mainly due to their charges which create repulsion and facilitate the nanofibrils liberation. Cationic CNF can also be produced via cellulose fibers reaction with EPTMAC (2,3-Epoxypropyl)trimethylammonium chloride). In this case, they display antimicrobial properties thanks to the amine quaternary grafted (Chaker & Boufi, 2015; Littunen et al., 2016; Saini et al., 2016). However, the main drawback of those classic chemical pretreatments resides in the use of toxic chemicals and complex procedures still difficult to industrialize.

Since 2013, new pretreatments have been developed in order to further increase the quality, with low energy consumption, produce greener CNF and impart new properties. For example, Ghanadpour et al. (Ghanadpour, Carosio, Larsson, & Wågberg, 2015) introduced negative charges on cellulose fibers thanks to the phosphorylation. Sulfite softwood pulp was impregnated with ammonium hydrogen phosphate and urea at 1 wt%, filtered to a solid content of 10 wt%, dried at 70°C and then cured at 150°C. Maximal charge of 1,8 mmol/g was measured and CNF of high quality with flame-retardant properties were produced via a microfluidizer. Phosphorylation of cellulose fibers for nanofibrillation is a very recent process which can lead to high-quality CNF, easily produced at industrial scale. Today, few publications are available. Naderi et al. (Naderi et al., 2016), used similar protocol without filtration step and using NaH₂PO₄. They showed that microfluidization is impossible under a degree of substitution of 0.13. Another protocol was proposed in 2017 by Noguchi et al. (Noguchi, Homma, & Matsubara, 2017) and allows reaching a charge content of 2.2 mmol/g.

82 Softwood pulp sheets were soaked in solution of $\text{NH}_4\text{H}_2\text{PO}_4$ and urea and then cured in hot air
83 at 165°C for 10 min. CNF of 3-4 nm wide and high transparency suspensions were produced
84 thanks to a homogenizer. The phosphorylation does not lead in change in crystallinity or
85 degree of polymerization (DP) of the cellulose fibers. Such good results have been even
86 transfer to industry with first production announcement in Japan (Yajima, 2018).

87 Even if phosphorylated CNF have appeared recently, cellulose phosphorylation is an old
88 and well-known process. Phosphorylated cellulose is used in many fields as for example
89 orthopaedics (Petreus et al., 2014), biomedical (Granja et al., 2001; Mucalo, Kato, &
90 Yokogawa, 2009), textiles (Davis, Findlay, & Rogers, 1949) or bio-chemical separation
91 (Suflet, Chitanu, & Popa, 2006). Phosphate groups can be introduced to cellulose during
92 homogeneous or heterogeneous reaction. In many papers, cellulose phosphorylation is done
93 on organic solvent such as pyridine (Reid & Mazzeno, 1949; Reid, Mazzeno, & Buras, 1949)
94 or dimethylformamide (Katsuura & Mizuno, 1966) using phosphorylating agents such as
95 phosphorus pentoxide, phosphoric acid or phosphate salt (Aoki & Nishio, 2010; Coleman et
96 al., 2011; Inagaki, Nakamura, Asai, & Katsuura, 1976; Reid et al., 1949). Microcrystalline
97 cellulose was also phosphorylated in molten urea as solvent using phosphorus acid (Suflet et
98 al., 2006). Cellulose can also be phosphorylated using water, urea and phosphoric acid/salts.
99 For example, Gallagher (Gallagher, 1965) soaked cotton fibers in phosphate salt solution
100 before heating at a temperature superior to 100°C for less than 15 min. Ichiwaka et al. (Patent
101 No. JP54138060A, 1979) used almost the same protocol but the curing step was longer (1-3h)
102 for obtaining fire retardant materials. Nuessle et al. (Nuessle, Ford, Hall, & Lippert, 1956)
103 phosphorylated cellulose by immersing fibers in a water/urea/diammonium phosphate system
104 followed by a curing step at 150°C for 10 min. In many papers, urea is used to enhance fiber
105 swelling and to prevent the degradation of cellulose during the curing step. Phosphorylation
106 of cellulose fibers in water based urea system using phosphate salts appears as the easier
107 process and it is the one classically used to produce CNF (Ghanadpour et al., 2015; Naderi et
108 al., 2016; Noguchi et al., 2017). However, only few papers tried to optimize this process and
109 understand the role of salts solubility parameter, their penetration and functionality.

110 The aim of this work is to optimize the phosphorylation of cellulose fibers in aqueous
111 media to increase the phosphorus content. For that, adsorption of different phosphate salts on
112 cellulose fibers was studied and phosphate salts with different constants of solubility were
113 tested. Position of phosphate group on the anhydroglucose unit and phosphorus penetration on
114 the fibers were also studied using ToF-SIMS, NMR and SEM-EDX.

115 2. Materials & methods

116 2.1 Materials

117 Cellulose used throughout this work is eucalyptus bleached kraft pulp Fibria T35. All the
118 materials and chemicals were used as received from the producers: urea (99.5%, Roth),
119 ammonium phosphate monobasic ($\text{NH}_4\text{H}_2\text{PO}_4$, >99%, Sigma Aldrich), ammonium phosphate
120 dibasic ($(\text{NH}_4)_2\text{HPO}_4$, >99%, Sigma Aldrich), lithium phosphate monobasic (LiH_2PO_4 , 99%,
121 Sigma Aldrich), sodium phosphate monobasic (NaH_2PO_4 , >99%, Sigma Aldrich), sodium
122 phosphate dibasic (Na_2HPO_4 , 99%, Sigma Aldrich), sodium hydroxide (NaOH, 99%, Sigma
123 Aldrich), hydrochloric acid (HCl, 37%, Sigma Aldrich). Distilled water was used for all the
124 preparations.

125 2.2 Methods

126 *Refining cellulose.* Cellulose fibers were dispersed in water at 2 wt% and refined using a pilot
127 disk beater (Matech, France) until reaching a Schopper-Riegler degree ($^{\circ}\text{SR}$) of about 90. At
128 least three measurements of $^{\circ}\text{SR}$ were done following standard ISO 5267.

129 *Phosphorylation of cellulose fibers.* Refined cellulose suspensions at different concentration
130 (1 wt%, 2 wt% or 5 wt% solid content) were mixed with different amount of urea and
131 phosphate salts ($\text{NH}_4\text{H}_2\text{PO}_4$, $(\text{NH}_4)_2\text{HPO}_4$, NaH_2PO_4 , Na_2HPO_4 , LiH_2PO_4) for 30 min. The
132 different ratio of AGU/ HPO_4 /urea used are 1/1.2/4.9, 1/0.32/1.29, 1/1.6/6.58, 1/3.22/12.88,
133 1/4.83/19.75 and it corresponds to a $(\text{NH}_4)_2\text{HPO}_4$ concentration of respectively 0.0744, 0.02,
134 0.1, 0.2, 0.3 mol/L. After that, suspensions at 1 and 2 wt% were filtered until 10 wt% and
135 dried at 105°C according to the protocol of Ghanadpour et al.(Ghanadpour et al., 2015). When
136 the test was made with a cellulose concentration of 5 wt%, fiber suspension was not filtered
137 but directly dried at 105°C . Finally, dried fibers were cured at 150°C for 1h in an oven. After
138 the curing step, fibers were soaked in water at 2 wt%, redispersed and washed several times
139 with boiling water and water under filtration with filter of $1\mu\text{m}$.

140 *Phosphorus content in the filtrate by pH titration.* When cellulose suspension (at 1 or 2 wt%)
141 was filtered until 10 wt% before the drying step, the concentration of phosphate groups in the
142 filtrate was measured. 200 mL of the filtrate was titrated with HCl at 0.5M. The phosphate
143 component reacts with acid to form phosphoric acid.

144 The concentration of phosphate salt in the filtrate is evaluated and the quantity of phosphate
145 ion adsorbed in mmol per gram of cellulose is then deduced. At least duplicates were
146 performed.

147 *Total charge content of phosphorylated fibers.* After the curing step and the washing step, the
148 phosphorylated pulp was titrated by conductivity with NaOH. 0.5 g (equivalent dry) of
149 modified cellulose fibers were dispersed in 200 mL of distilled water and the pH was reduced
150 to 3 to convert the hydroxyl groups in their acidic form. The total charge content is measured
151 by titration using NaOH 0.05M. At least triplicates were performed.

152 *Elemental analysis & ICP analysis.* Carbon, hydrogen, oxygen and phosphorus contents were
153 measured for the different phosphorylated cellulose pulps using a Vario MICRO cube CHNS-
154 O elemental analyzer (Elementar). Phosphorus total content was measured after micro waves
155 mineralization in presence of acid and followed by inductively coupled plasma (ICP). At least
156 two measurements were done for each sample. The degree of substitution was calculated on
157 the basis of the phosphorus content using the following equation:

158
$$DS = \frac{162 * \%P}{n_{P \text{ in grafted mol.}} * M(P) - M(\text{grafted mol.}) * \%P}$$

159

160 where %P is the P content determined by ICP, M(P) is the molar mass of phosphore (i.e. 31
161 g/mol), M(grafted mol.) is the molar mass of the grafted molecule (i.e. 80 g/mol) and $n_{P \text{ in}}$
162 $_{\text{grafted mol.}}$ is the number of P element in the grafted molecule.

163 *Degree of polymerization (DP) of cellulose fibers.* DP was evaluated using the ISO 5351:2010
164 standard. 250 mg (equivalent dry) of phosphorylated cellulose fibers was dissolved in copper
165 (II) ethylenediamine and intrinsic viscosity ($\eta_{\text{int.}}$) was measured at least three times. The
166 degree of polymerization (DP) was calculated using the Mark-Houwink-Sakurada equation
167 and the intrinsic viscosity as follows:

168
$$DP^{0.905} = 0.75 \eta_{\text{int.}}$$

169 At least duplicates were performed.

170 *Crystallinity Index (CI).* CI of the modified celluloses was obtained using wide-angle X-ray
171 diffraction (XRD) spectra. A PANalytical X'Pert PRO MPD diffractometer, equipped with

172 an X'celerator detector was used and X-rays were generated with a copper anode (K α
173 radiation $\lambda = 1.5419 \text{ \AA}$). The cellulose CI (%) was determined according to the peak height
174 method, where I_{002} represents the diffraction intensity of the main crystalline peak at $2\theta \approx$
175 22.5° and I_{am} is the intensity at $2\theta \approx 18.7^\circ$. All the samples were tested at least in duplicate.

$$176 \quad CI = \frac{(I_{002} - I_{am}) * 100}{I_{002}}$$

177 *Optical microscopy images.* Cellulose suspensions were diluted to 0.5 wt% and optical
178 microscopy images were taken. A Carl Zeiss Axio Imager M1 (Germany) optical microscope
179 was used in a transmission mode. A minimum of five pictures were taken for each sample and
180 the most representative is shown here.

181 *Scanning Electron Microscopy – Energy Dispersive X-ray analysis (SEM-EDX).* Scanning
182 electron microscopy equipped with an energy-dispersive X-ray spectroscopy module (LEO
183 Stereoscan 440). Detector Si (Li) EDAX-10 mm² was used to evaluate the position of
184 phosphate groups in the fiber. Tension was reduced at 6 keV and the acquisition time was
185 2h30 in order to increase the resolution.

186 *X-Ray photoelectron spectroscopy (XPS).* Chemical analysis was also established for the
187 modified and unmodified samples. The test was carried out using a K α apparatus modulated
188 with a monochromatic Al K α X-ray source at 14,875 eV. The substrates were positioned at an
189 angle of 90° under an ultrahigh vacuum of less than 10^{-7} Pa. Spectrum NT was used to
190 decompose the signal and the overall spectrum was shifted to fix the contribution of C-C in
191 the C_{1s} spectra at 285.0 keV.

192 The O/C ratio was calculated using the following equation:

$$193 \quad \frac{O}{C} = \frac{I_O}{S_O} * \frac{S_C}{I_C}$$

194 where I_O and I_C are the intensity of the oxygen and carbon peaks respectively. S_C , S_O and S_P
195 are equal to 0.00170, 0.00477 and 0.0014 for carbon, oxygen and phosphorus respectively. It
196 characterizes the atomic sensitivity factor. P/C ratio was also calculated using this method.

197 *Nuclear Magnetic Resonance (NMR).* Solid-state NMR experiments were performed on
198 Bruker Avance III HD 11.75 T spectrometer equipped with a 3.2 mm triple resonance low
199 temperature MAS probe and Bruker Avance Neo 21.14 T spectrometer equipped with a 1.3
200 mm triple resonance MAS probe in double resonance mode. The ¹³C detected ¹H-¹³C CP, ¹H-

201 ^{13}C HETCOR, 1D ^1H CRAMPS and 2D ^1H DQ-CRAMPS experiments for all the samples
202 were carried out on Bruker Avance III HD 11.75 T spectrometer using magic angle spinning
203 (MAS) of 12.5 kHz. The proton detected ^{13}C - ^1H HETCOR and ^1H DQMAS experiments were
204 performed for all the samples on Bruker Avance Neo 21.14 T spectrometer using MAS rate of
205 62.5 kHz. The proton and carbon spectra were referenced externally by using L-alanine
206 methyl proton as 1.38 ppm and methyl carbon as 20.5 ppm. All the experiments were
207 performed at room temperature.

208 *Time of Flight-Secondary Ion Mass Spectrometry (ToF-SIMS)*. This technique makes possible
209 the molecular structures identification at the top surface of materials (information depth
210 limited to a few monolayers i.e. about 2 to 5nm) and was used here to gain more insight on
211 the grafting mode of the phosphorylation at the surface of the fibers. Measurements were
212 carried out on a TRIFT III ToF-SIMS instrument from Physical Electronics operated with a
213 pulsed 22 keV Au^+ ion gun rastered over a $300 \times 300 \mu\text{m}^2$ area. Data were analyzed using the
214 WinCadence software. Mass calibration was performed on hydrocarbon secondary ions. The
215 relative intensity for a given ion was calculated by dividing the intensity of that ion by the
216 total integrated intensity minus the H intensity which is barely reproducible.

217 **3. Results & discussions**

218 **3.1 Effect of the filtration step on the final charge content of the modified fibers**

219 The objectives of this part are to check if there is adsorption of phosphate ions and to
220 evaluate the influence of the filtration step on the final charge content.

221 Cellulose fiber suspensions at 1 wt% were mixed with $(\text{NH}_4)_2\text{HPO}_4$ and urea in quantity
222 described in Methods part and then filtered until 10 wt%. The filtrate was pH titrated in order
223 to measure the non-absorbed phosphate groups and so deduced the charge adsorbed.

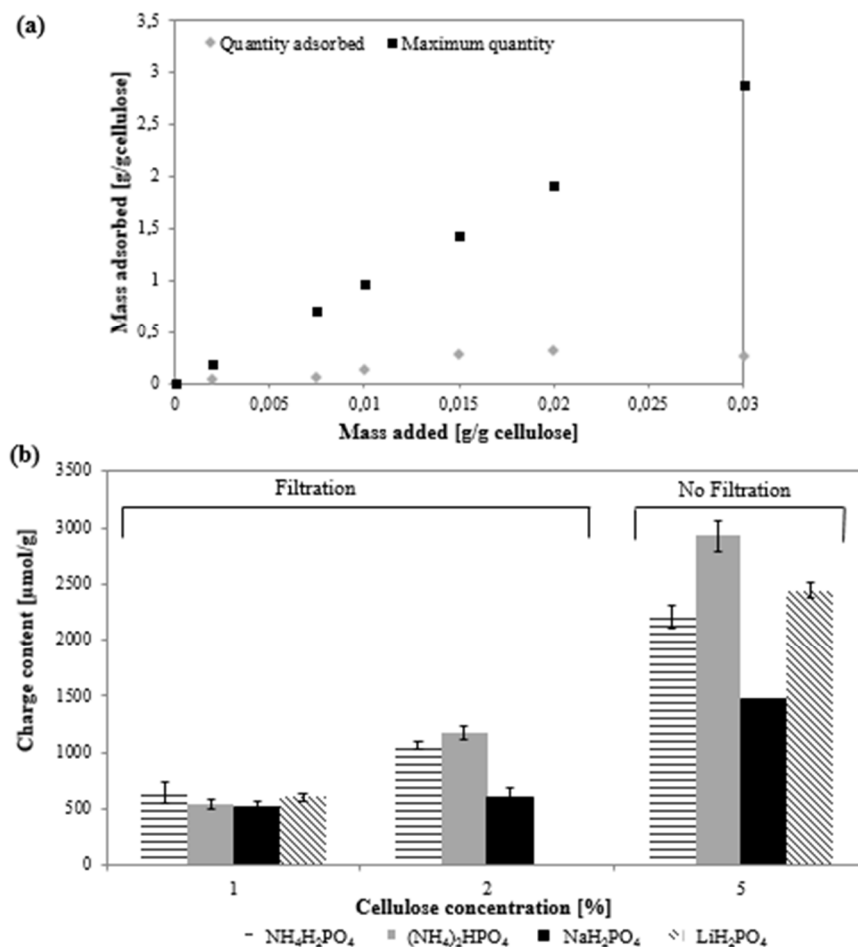


Figure 1: Phosphorylation of cellulose fibers (a) adsorption of phosphore depending on mass of phosphate salt added and (b) depending on cellulose concentration and phosphate salt

224 Salt adsorption increases with the concentration of phosphate salt as shown in Figure 1a.
225 However, the mass adsorbed was very low compared to the mass added. Cellulose fibers
226 which are slightly negatively charged (0.06 mmol/g) due to residual hemicelluloses or
227 cellulose oxidation during bleaching constitute heterogeneous surface and are not favorable to
228 adsorb anionic phosphate salt. Phosphate compound is poorly adsorbed on cellulose fibers and
229 the filtration step before the drying step eliminates most of the salt.

230 Cellulose concentration and the effect of the filtration step were then studied as reported in
231 Figure 1b. The final charge content increases a lot with the cellulose concentration and was
232 really higher when the filtration step was eliminated whatever the phosphate salts. When
233 cellulose pulp was at 2 wt% solid content, phosphate groups were “closer” to the fibers than at
234 1 wt% and the adsorption step before the filtration might be improved and so the final charge
235 content. Another explanation is the fibers entanglement. At 2 wt% entanglement was
236 increased and phosphate salts were trapped easily in the fibrous mat during the filtration. Both
237 options result in higher modification rate.

238 When phosphorylation occurs, fiber swells and may even be dissolved as reported by
239 Ghanadpour et al.(Ghanadpour et al., 2015) and confirmed by optical microscopy in Figure
240 S4. We supposed that phosphorylation starts at the fiber surface and then thanks to the
241 swelling, phosphate salts can reach the core of the fibers. When phosphate ion was just
242 adsorbed on the surface, charge content was lower. On the contrary, when filtration step was
243 eliminated, excess of phosphorus was present and the phosphorylation can go further from the
244 surface to the core. This fact is confirmed by Noguchi et al.(Noguchi et al., 2017) who
245 obtained higher charge content using high cellulose concentrated medium and lower
246 phosphate salt concentration (ratio 1/0.63/3.22 compared to a ratio of 1/1.2/ 4.9 with
247 filtration). Eliminating the filtration step constitutes a good option to increase the charge
248 content without increasing the chemicals consumption.

249 **3.2 Urea role during the phosphorylation of cellulose fibers**

250 Urea has already been used in many protocols to prevent the degradation of cellulose
251 (Ghanadpour et al., 2015; Noguchi et al., 2017; Nuessle et al., 1956; Suflet et al., 2006), to act
252 as a catalyst (Lagier, Zuriaga, Monti, & Olivieri, 1996; Yurkshtovich, Yurkshtovich,
253 Kaputskii, Golub, & Kosterova, 2007) or to enhance the fibers swelling and hence increase
254 the phosphate groups penetration. Urea effect was investigated as reported in Table 1.

Table 1: Influence of urea content in cellulose phosphorylation

Cellulose concentration	Molar ratio AGU/ (NH ₄) ₂ HPO ₄ / Urea	Charge content [mmol/g]	Cellulose color	Presence of aggregate
2	1/0/0	0.06 ± 0.01	White	No
2	1/0/4.9	0.17 ± 0.03	White	No
2	1/1.2/0	0.37 ± 0.01	Black	Yes
2	1/1.2/4.9	1.18 ± 0.06	Brown	Yes
2	1/1.2/7.2	2.37 ± 0.05	Yellow	Yes

256 Without urea, the phosphorylation only slightly occurs with a charge content of 0.37
 257 mmol/g whereas the cellulose became totally black. It is now clear that urea is necessary to
 258 phosphorylated cellulose but also to prevent cellulose degradation. One reactional mechanism
 259 adapted from Kokol et al.(Kokol, Božič, Vogrinčič, & Mathew, 2015) is presented in Figure 2
 260 with several phosphorylated cellulose structure possibilities. Urea has an active role in the
 261 reaction but also in the protection of the cellulose. Presence of nitrogen basic elements in the
 262 phosphorylation process seems primordial (Katsuura & Mizuno, 1966; Nuessle et al., 1956;
 263 Reid & Mazzeno, 1949; Reid et al., 1949).

264 When urea content increased, charge content increased and the coloration of cellulose
 265 decreased. Yurkshtovich et al.(Yurkshtovich et al., 2007) showed that phosphorus content
 266 increased with the concentration of urea up to 3.33M (i.e. 4 times higher than what we used
 267 here). However side reaction can occur and creates carbamate. This is not a problem from a
 268 nanofibrillation point of view, because it also weakens the H-bonds between cellulose
 269 nanofibrils.

270 3.3 Influence of phosphate salt solubility and pH on the final charge content

271 Up to our knowledge, no study dedicated to phosphorylated CNF has compared various
 272 phosphate salts. In this study, higher modification rates were expected with an higher constant
 273 of solubility (Ks). Unfortunately, no relationship between the degree of substitution and the
 274 Ks was observed even if various phosphorylation rates are clearly obtained, depending on the
 275 phosphate salt Ks as reported on Table 2. However, if the Ks is very low (for example
 276 Na₂HPO₄), the grafting was very low. Indeed, the counterion was closer due to lower
 277 dissociation and there was some hindrance and less reactivity.

278 For a same counterion, the total charge content increased if the Ks increased, meaning that
 279 counterion have more impact than Ks. In each case, the counterion ammonium (NH₄⁺) led to

280 higher DS than lithium (Li^+) and than sodium (Na^+). For now, counterion effect in the
 281 chemical reaction is still under discussion (Manet, 2007). Some studies reported that in
 282 concentrated sodium hydroxide media, NH_4^+ have a lower affinity with hydroxyl groups and
 283 will not surround the anhydroglucose units. Moreover, the ammonium counterion has a lower
 284 affinity for water than sodium ion. The more hydrophobic character of NH_4^+ would produce
 285 more pronounced swelling of the cellulose as the non-activated anhydroglucose unit will be
 286 repelled (Ott, Spurlin, Grafflin, Bikales, & Segal, 1954). In water, lithium ion is more
 287 hydrated than sodium followed by ammonium. Counterion electronegativity can also
 288 influence the reaction. Lithium and sodium with an electronegativity of respectively 0.98 and
 289 0.93 are much less electronegative than nitrogen (3.04) and so the quaternary ammonium. The
 290 distance between NH_4^+ and HPO_4^{2-} is longer than the one between Li^+ or Na^+ and HPO_4^{2-} due
 291 to lower difference of electronegativity. NH_4^+ is more distant of HPO_4^{2-} than the other
 292 counterion and so salts are less stable (or more reactive) which leads to higher grafting.

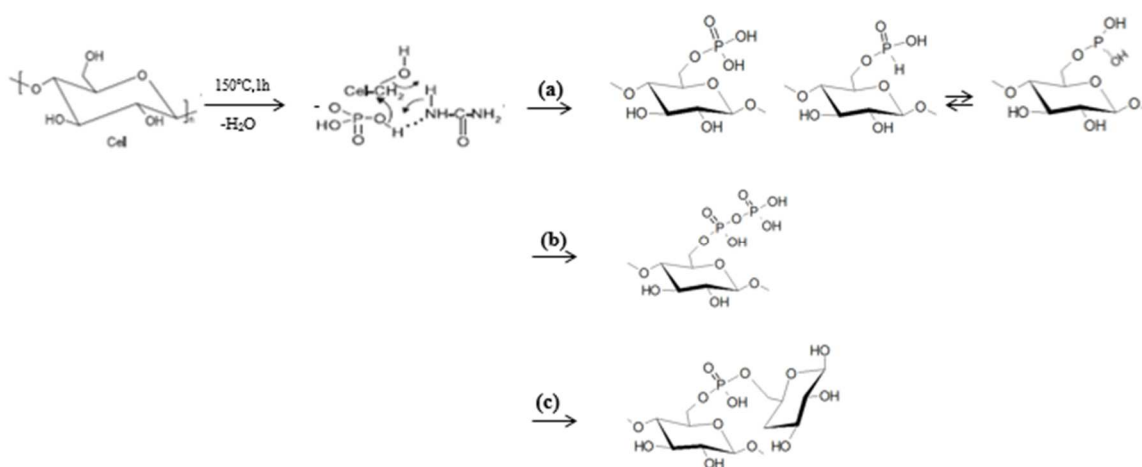
293 **Table 2:** Influence of phosphate salt constant of solubility (Ks) and pH, on cellulose
 294 phosphorylation using AGU/Phosphate salt/ urea ratio of 1/1.2/4.9 and cellulose fiber
 295 concentration of 5 wt% without filtration. *pH was modified by adding NaOH or HCl

Phosphate salt	Ks	Cellulose concentration [%]	pH	Charge content [mmol/g]	Equivalent DS	DS based on P content [AE]
LiH_2PO_4	126	5	9*	2.15 ± 0.31	0.35	-
LiH_2PO_4	126	5	5	2.44 ± 0.07	0.39	0.18
NaH_2PO_4	94.9	5	10*	0.48 ± 0.12	0.08	-
NaH_2PO_4	94.9	5	4	1.48 ± 0.12	0.24	0.29
$(\text{NH}_4)_2\text{HPO}_4$	68.9	5	8	2.93 ± 0.14	0.47	0.45
$(\text{NH}_4)_2\text{HPO}_4$	68.9	5	4*	4.40 ± 0.50	0.71	-
$\text{NH}_4\text{H}_2\text{PO}_4$	37.4	5	4	2.21 ± 0.10	0.36	-
Na_2HPO_4	12	5	8	0.41 ± 0.01	0.07	-

296 The pH effect was also investigated. For every phosphate salt, the reactivity and the final
 297 charge content was higher when acidic medium was used as confirmed by Lim and Seib on
 298 wheat starch (Lim & Seib, 1993). For example, charge content passes from 0.5 to 1.48
 299 mmol/g for NaH_2PO_4 or from 2.93 to 4.40 for $(\text{NH}_4)_2\text{HPO}_4$. Indeed at acidic pH, two OH
 300 groups are available on the phosphate salt and the reaction is improved. Moreover, in acidic
 301 medium, negative charges of cellulose are reduced and anionic phosphates are not repelled.

302 3.4 Chemical structure of the grafted cellulose fibers

303 As shown in the Figure 2, different cellulose structures can be obtained after the
304 phosphorylation. Hydroxyl groups of cellulose can react with phosphate salt and form
305 phosphate groups (Cell-O-P(O)(OH)₂), phosphite groups (Cell-O-P(OH)₂) or combination.
306 Crosslinking can also occur (Noguchi et al., 2017). Some aggregates are formed during the
307 curing step and are really difficult to destroy and might correspond to crosslinked structures.
308 Moreover, position of phosphate groups on the cellulose units and its penetration on the fiber
309 is not so evident. Different methods were investigated to determine which form is the
310 preferential one and how fibers are modified.



311 **Figure 2:** Different grafting modes for phosphorylated cellulose as proposed by Kokol et
312 al.(Kokol et al., 2015)

313 3.4.1 Conductivity titration

314 The first method that might give information about the cellulose structure is the
315 conductimetric titration (Figure S1). The degree of substitution measured by elemental
316 analysis is equal to the one obtained by conductimetric titration as reported in Table 2 and
317 confirmed by Naderi et al.(Naderi et al., 2016). During the titration only one pH jump is
318 observed meaning that only one hydroxyl group is titrated. This can suppose that the
319 phosphate group form is the one in Figure 2a, (second form) or that there is crosslinking like
320 in scheme Figure 2c. However Kokol et al.(Kokol et al., 2015) reported pK_a of 6.8 and 12.5
321 for (Cell-O-PO₃H₂/ Cell-O-PO₃H⁻) and cell-CH₂-O-PO₃²⁻. Most of the time the titration was
322 done between pH 2 and 11 meaning that the second hydroxyl groups of the phosphate group
323 is not measured which means that all the form presented in Figure 2 could be obtained.

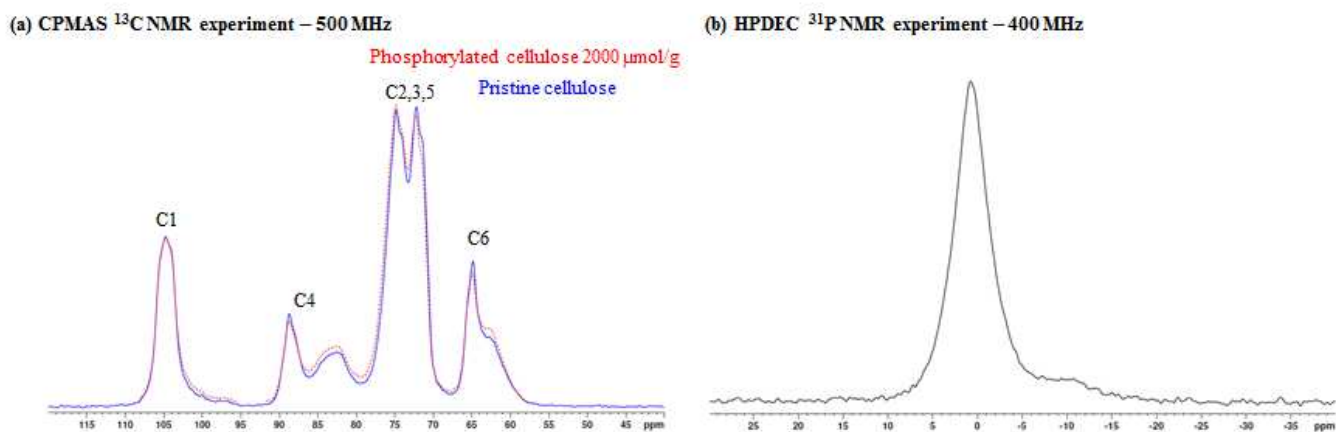
324 However, even when the pH was increased until 13 for some trials, only one pH jump was
325 reported.

326 **3.4.2 Solid-State NMR**

327 *High-resolution solid-state NMR at 11.74 Tesla*

328 Native and phosphorylated cellulose fibers were analyzed at 11.74 T (500 MHz for ^1H
329 resonance) using ^{13}C , ^{31}P and ^1H NMR analyses as reported in Figures 3 and 4 to determine
330 where the phosphorus is located. The ^{13}C NMR spectrum is shown in Figure 3a. The
331 respective spectra of cellulose and phosphorylated cellulose are consistent with the data
332 reported in the literature. The peak in the 58-68 ppm region corresponds to the C6 of the
333 cellulose ring, in 68-80 ppm region to C2, C3 and C5 carbon, from 80 to 91 ppm to the C4
334 and finally from 101 to 109 ppm to the C1 (Atalla & Vanderhart, 1984). Note that signals at
335 84 ppm and 63 ppm are respectively assigned to C4 and C6 of amorphous domains of
336 celluloses (Atalla & VanderHart, 1999; Montanari, Roumani, Heux, & Vignon, 2005). As
337 their spectra appear to be very alike, it indicates that the carbon structure of the
338 phosphorylated cellulose fibers with a charge content of 2.10 mmol/g might be not
339 significantly modified compared to the carbon structure of the pristine cellulose. Ghanadpour
340 et al.(Ghanadpour et al., 2015) also reported that all the regions of modified fibers are slightly
341 changed and thus no region selectivity is observed. In our case, it could indicate that the
342 phosphate grafting was homogenously distributed on the cellulose fibers which do not lead to
343 specific changes in the ^{13}C chemical shift.

344 The presence of phosphorus on the cellulose fibers after a strong washing step is confirmed
345 by an intense signal in the HPDEC ^{31}P NMR spectra as shown in Figure 3b. The phosphorus
346 components appeared in the region -10 to 10 ppm it is mainly made of an intense signal at 0
347 ppm overlapping a broader low intensity signal which spreads down -15 ppm.



348 **Figure 3:** Influence of the phosphorylation on the carbon structure of the cellulose: (a) ^{13}C
 349 solid-NMR spectra and (b) HPDEC ^{31}P

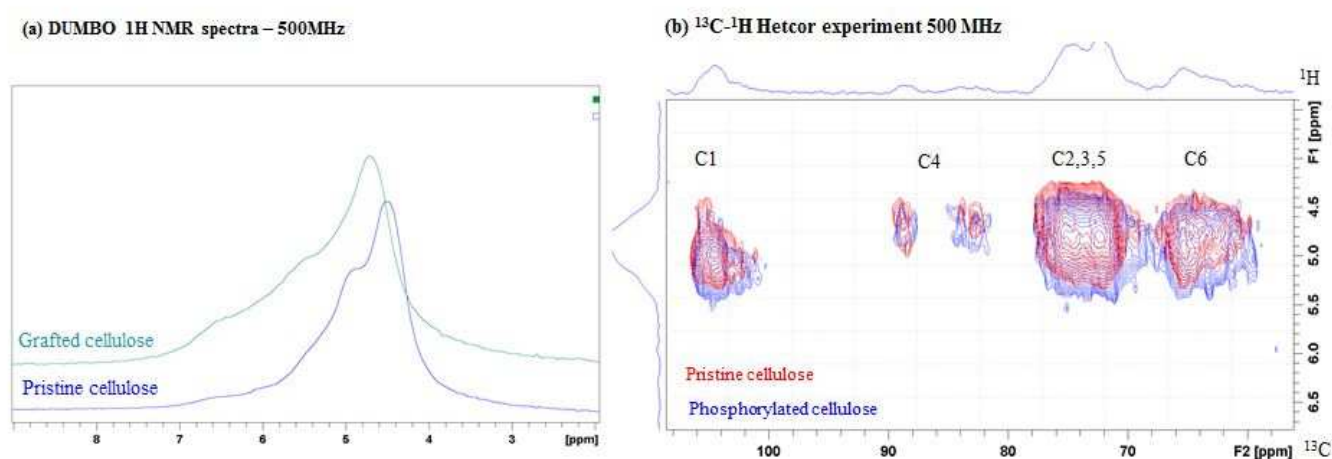
350 At a 11.7 T field high-resolution solid-state ^1H NMR spectra of both pristine and
 351 phosphorylated cellulose were obtained with DUMBO sequence and reported in Figure 4a.
 352 Very interestingly, contrarily to their carbons counterparts the proton spectra present some
 353 significant differences. We can observe a low shift of the maximum intensity from pristine to
 354 grafted celluloses. Moreover, the spectra of the grafted cellulose present two large and intense
 355 shoulders between 5 and 7 ppm. Similar signals are also observed in the pristine cellulose but
 356 much less intense. It means that new type of protons appeared during the phosphorylation.
 357 Those new protons can be due to either (i) hydroxyl protons at the phosphate groups grafted
 358 on cellulose or (ii) modifications of the hydrogen bond network. This latter statement can be
 359 supported by the number of oxygens, brought by the phosphorylation, that are good candidate
 360 to modify the hydrogen bond network. As protons resonances are shifted to the high
 361 frequencies we can infer that the amount of proton involved in hydrogen bond network is
 362 increased.

363 To have more information concerning the proton network of the phosphorylated and
 364 pristine celluloses, dipolar proton-carbon correlation experiments were carried out and
 365 reported in Figure 4b.

366 The 2D maps (normalized related to the intensity of signals of crystalline C4) look very
 367 similar, however some differences can be noticed. In Figure 4b, showing the dipolar
 368 interactions between C and H, the proton resonances of the phosphorylated cellulose are
 369 shifted to the higher frequency except the protons in interaction with C4 of crystalline

370 domains. Due to the normalization, it appears that the amount of C4 in amorphous domain is
371 increased (larger correlation). In a similar way the correlation assigned to C2,3,5 appears to be
372 broader in the phosphorylated cellulose than in the pristine one. The correlation at C1 is not
373 significantly affected.

374 On the base of the expected chemistry of phosphorylation, grafting should occur mainly at
375 C6. Therefore the broadening that we mentioned previously of C2,3,5 correlations at around
376 68 ppm could be assigned not to chemical shift changes of these carbons but mainly to the
377 effect of substitution on C6 which leads to a low field effect and consequently to the observed
378 signal broadening of C2,C3,C5 correlation. Moreover grafting mainly appears on amorphous
379 domain (increase of the amorphous C4).

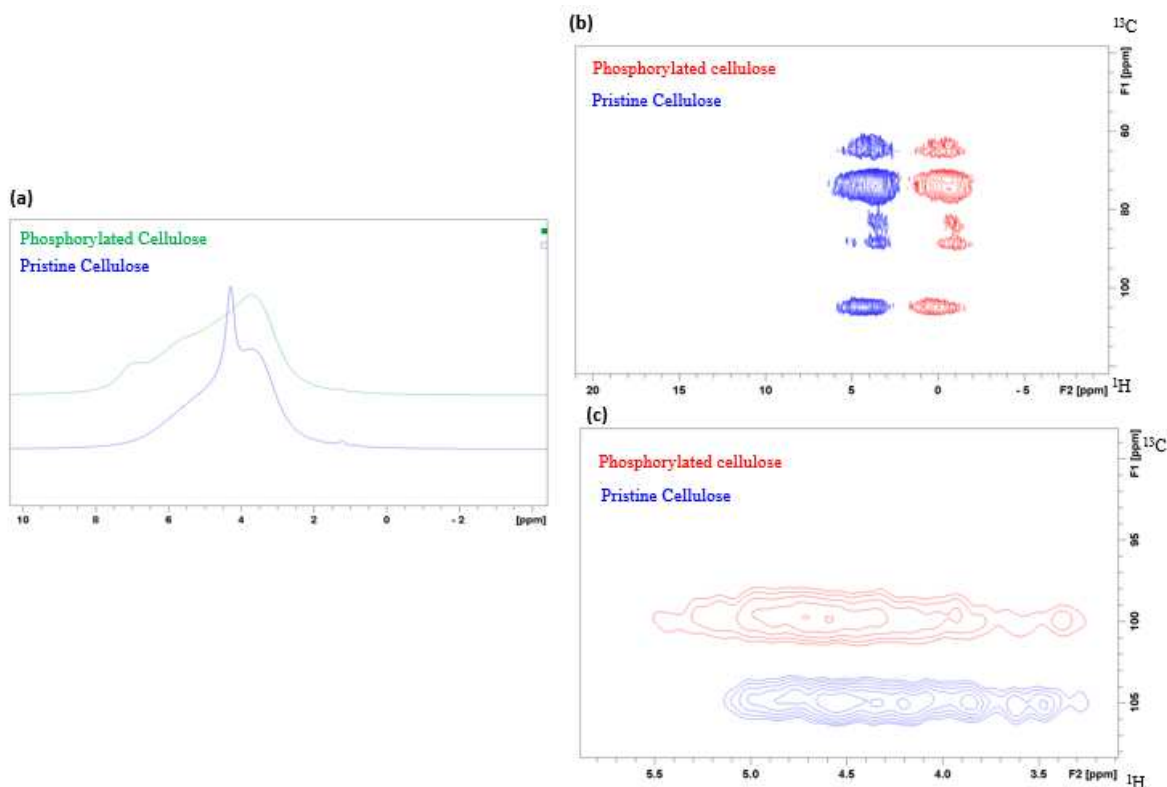


380 **Figure 4:** Solid-NMR spectra. Effect of the phosphorylation on the proton network of
381 cellulose fibers. (a) Hetcor experiment and (b) DUMBO experiment

382 *High-resolution solid-state NMR at 21.1 Tesla*

383 The spectra recorded at 21.1 T with MAS rate of 62.5 KHz bring some complementary
384 information. On an experimental point of view, to the fact that very high spinning rates are
385 used, some consequences are expected. For ^1H NMR, spectra can be acquired either with
386 direct excitation or with spin echo experiment. For the dipolar ^1H - ^{13}C correlation experiments
387 (proton detected at this field), it has to be mentioned that due to the high spinning rate of the
388 samples the molecular domains with small proton carbon dipolar interactions can be difficult
389 to detect. In that case the experiment enhances the crystalline parts of pristine or
390 phosphorylated celluloses. Taking into account these observations the following conclusions
391 can be drawn.

392 The ^1H NMR recorded at 21.1 T and shown in Figure 5,a confirms the results obtained at
 393 11.7 T, namely the presence of new signals at 5 and 7 ppm. Note that for the pristine cellulose
 394 the signal at 4.2 ppm is assigned to water molecules which can be identified by adding small
 395 quantity of water to the sample and which are very sensitive to the temperature.

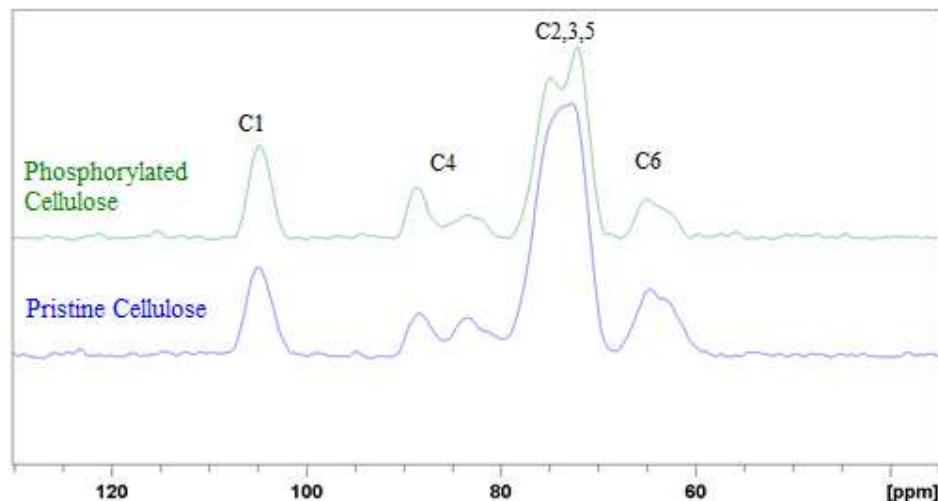


396 **Figure 5:** (a) ^1H NMR recorded at 21.1T for pristine cellulose and phosphorylated cellulose;
 397 (b) and (c) Proton-carbon correlation recorded at 21.1 T. Influence of the phosphorylation on
 398 the cellulose structure

399 Contrary to the 2D ^1H - ^{13}C correlation experiments recorded at 11.7 T the 2D spectra
 400 recorded at 21.1 T are very similar, as shown in Figure 5b,c . It has to be reminding that in
 401 that case we mainly see the crystalline domain of the materials. However the C1 are
 402 correlated to protons that appear to be slightly shifted at higher frequency in the
 403 phosphorylated cellulose compared to pristine.

404 At such field, due to the fast spinning rate and the low amount of material that are analyzed
 405 in the order of a few mgs, direct detection of ^{13}C NMR is impossible within reasonable
 406 experiment time. The only way to obtain an equivalent 1D spectrum is to calculate the sum of
 407 the columns (carbon in the indirect dimension). The calculated spectra are shown in Figure 6
 408 and contrary to the ^{13}C spectrum acquired at 11.7 T the spectra present some differences. The

409 feature of the calculated spectrum of phosphorylated cellulose appears to be more crystalline
410 than the pristine one. It is a strong indication that the phosphorylation of cellulose fibers lead
411 to amorphous domains which are not seen in the 2D experiments recorded under these
412 conditions, i.e., 21.1 T and 62500 Hz of spinning rate.



413 **Figure 6:** Reconstituted ^{13}C NMR 1D spectrum of pristine cellulose and phosphorylated
414 cellulose

415 To conclude, the NMR analysis cannot help to determine which exact structure of the
416 phosphorylated cellulose fiber is formed insofar as the carbon structure is not affected and the
417 proton network is entirely modified. However, the phosphorylation is clearly visible regarding
418 the ^{31}P spectrum or with the change in the proton network.

419 3.4.3 Time of Flight-Secondary Ion Mass Spectrometry

420 ToF-SIMS analyses were performed at the surface the phosphorylated cellulose fibers to try
421 to determine the preferential grafting mode of phosphorylation at the extreme surface of
422 cellulose fibers. Results are displayed in Figures 7 and S2 and relative intensities of specific
423 signatures are given in Figure S3.

424 The phosphate salt, $(\text{NH}_4)_2\text{HPO}_4$, used for the phosphorylation of cellulose was analyzed in
425 its original form and several characteristics peaks were found: in the negative mode, PO_2^-
426 ($m/z = 62.96$), PO_3^- ($m/z = 78.96$) and H_2PO_4^- ($m/z = 96.97$) which are the typical peaks
427 detected for phosphorylated compounds but also HP_2O_6^- ($m/z = 158.93$), $\text{H}_3\text{P}_2\text{O}_7^-$ ($m/z =$
428 176.93) and $\text{H}_5\text{P}_2\text{O}_8^-$ ($m/z = 194.95$) and in the positive mode, $\text{NH}_3\text{H}_3\text{PO}_4^+$ ($m/z = 116.01$).

429 The peaks at $m/z = 120.96$ and 142.95 in the positive mode correspond to $\text{NaH}_3\text{PO}_4^+$ and
430 $\text{Na}_2\text{H}_2\text{PO}_4^+$, respectively, and indicate a cationization effect related to Na (a significant
431 intensity is also detected for Na^+). The detection of HP_2O_6^- ($m/z = 158.93$), $\text{H}_3\text{P}_2\text{O}_7^-$ ($m/z =$
432 176.93) and $\text{H}_5\text{P}_2\text{O}_8^-$ ($m/z = 194.95$) indicates a dimer alike based emission.

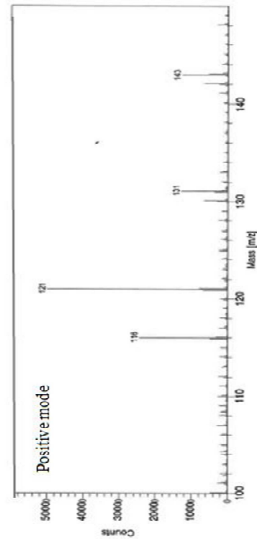
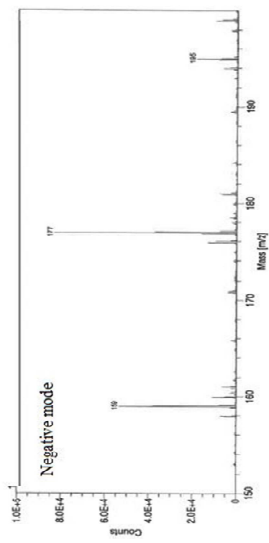
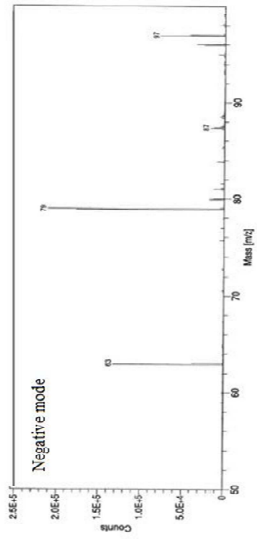
433 In the spectra of phosphorylated fibers, there was no detection of high mass molecular
434 peaks combining cellulose and the grafted moieties. On the other hand, no new phosphorus-
435 based secondary ions were detected.

436 In the positive mode spectra of phosphorylated fibers, the peak at $m/z = 116.01$
437 corresponding to $\text{NH}_3\text{H}_3\text{PO}_4^+$ was not detected, which can confirm the grafting as well as an
438 efficient washing step. Furthermore, urea displays a characteristic peak around at $m/z = 61.03$,
439 as shown in Figure S2, and this peak is not detected on the phosphorylated fibers meaning that
440 the washing step was efficient.

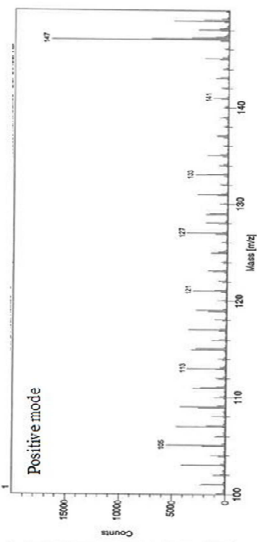
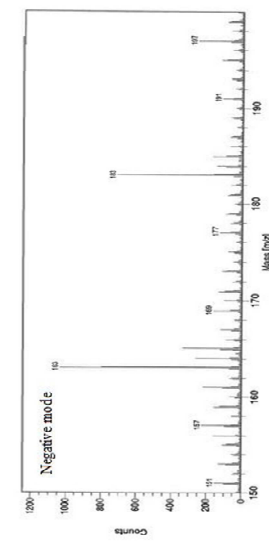
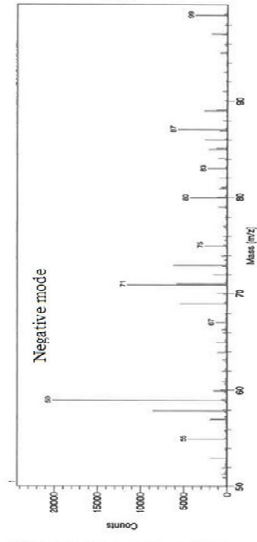
441 The spectra of phosphorylated fibers in the negative mode show some signatures of the
442 reference powder. PO_2^- ($m/z = 62.96$), PO_3^- ($m/z = 78.96$) and H_2PO_4^- ($m/z = 96.97$) are
443 detected in the modified cellulose fibers but their relative intensities are different for the
444 various samples (see Figure 7 and S3). Hence, a detailed study of the relative intensity of the
445 above described secondary ions was undertaken.

446 The relative intensities of PO_2^- , PO_3^- and H_2PO_4^- are similar for the phosphorylated pulps
447 with charge contents of 2.93 and 1.18 mmol/g (taking into account standard deviations) but
448 they are significantly different for the charge content equal to 0.54 mmol/g. This indicates a
449 different extent in the way of grafting, observed as a function of the different quantity of
450 phosphate salt added in the suspension. On the other hand, intensities are also different in the
451 spectra of the modified celluloses and in the spectra of the reference powder, which could
452 then help understanding what is the probable referred grafting mode among those displayed in
453 Figure 2. One must still be careful as no reference sample of the proposed grafting modes
454 could be available for ToF-SIMS analysis.

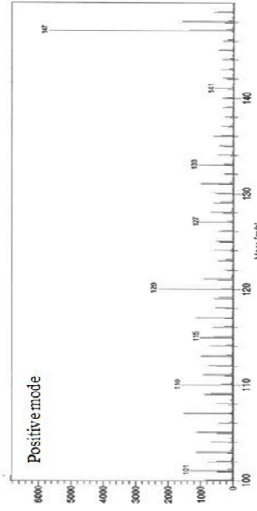
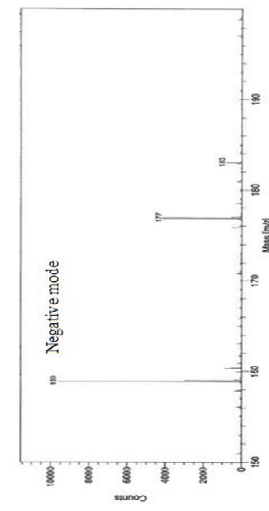
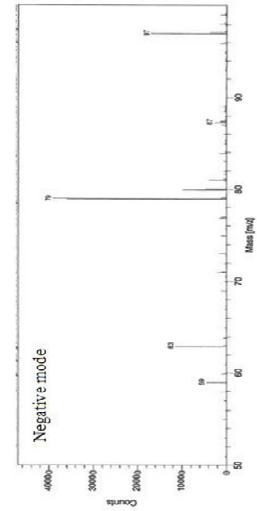
(NH₄)₂HPO₄ – powder



Cellulose



Phosphorylated cellulose



455 **Figure 7:** ToF-SIMS spectra of phosphate salt powder, pristine cellulose and phosphorylated
456 cellulose fibers in the positive in the 100-150 m/z range and in the negative modes in the 50-
457 100 and 150-200 m/z range

458 PO_3^- (m/z = 78.96) and H_2PO_4^- (m/z = 96.97) are the most preponderant secondary ions for
459 the modified fibers and their normalized intensity (according to PO_2 intensity) decreased
460 when grafting rate decreases. This can confirm that most of the phosphorylated fibers are in
461 the form of Figure 2a.

462 Moreover, the peaks at HP_2O_6^- (m/z = 158.93), $\text{H}_3\text{P}_2\text{O}_7^-$ (m/z = 176.93) are detected in the
463 phosphorylated cellulose fibers (the peak at m/z = 194.95 m/z exhibits a very low relative
464 intensity) but their relative intensities are really different, even between the samples with
465 charge contents of 2.93 and 1.18 mmol/g. The presence of this species increases with the
466 charge content from 0.54 to 2.93 mmol/g whereas the intensities of PO_2 , PO_3 and H_2PO_4
467 increase for a charge content from 0.5 to 1.1 and then tend to stabilize.

468 Those species can be present due (i) to the grafting of the impurities of the phosphate salt
469 powder on the fibers, (ii) due to the grafting of two HPO_4^{2-} ions on the cellulose, (iii) due to
470 the grafting of this species present in the powder on the cellulose fibers or due to (iv) possible
471 recombination during the analysis.

472 Their intensities in the functionalized fibers are different and this can be explained by
473 different reasons. First, if HPO_4^{2-} is grafted on the fibers, the combinations are less possible
474 and those species cannot be formed. HPO_4^{2-} is not free and cannot make combination.
475 However, in this case, if all the HPO_4^{2-} were grafted, the peaks at 158.93 and 176.93 m/z
476 would have totally disappeared. The presence of these two peaks at 158.93 and 176.93 m/z
477 can also relate the grafting of those species present in the powder or the combination of two
478 HPO_4^{2-} and formation of di or tri ester as reported in Figure 2b. The formation of the cellulose
479 structure described in Figure 2c should lead to new peaks and none are visible.

480 To conclude, no characteristic peak of the phosphorylated cellulose has been clearly
481 identified by ToF-SIMS analysis but some hypothesis of grafting was determined. It seems
482 that the phosphorus is present on the cellulose fiber with the H_2PO_4^- form and in a fewer
483 extent HP_2O_6 . The presence of crosslinked cellulose structures has been discarded insofar as
484 no signal was detected. This technique analyzes the extreme surface whereas some phosphate

485 salt can penetrate. That is why an intermediate surface technique (XPS) was performed to
486 carry on investigations.

487 **3.4.4 X-ray photoelectron spectroscopy**

488 The phosphorylated pulp with a charge content of 2.10 mmol/g and the pristine cellulose
489 were analyzed as reported in Figure S4. Total spectra of native and phosphorylated cellulose
490 are presented in Figure S4a. Distinct peaks of C_{1s} and O_{1s} are present on the native cellulose
491 as well as minor peaks characteristics of surface contamination. Additional peaks are present
492 on the phosphorylated cellulose. The peaks characteristics of the phosphorus appeared at
493 134.4 eV and 190.5 eV and are assigned to P_{2p} and P_{2s} (Božič, Liu, Mathew, & Kokol, 2014;
494 Ghanadpour et al., 2015; Pasqui, Rossi, Di Cintio, & Barbucci, 2007), confirming the
495 phosphorylation. The peak at 401.4 eV corresponds to the presence of nitrogen (Bourbigot, Le
496 Bras, Gengembre, & Delobel, 1994) N_{1s} which is probably assigned to NH₄⁺ groups of the
497 phosphate salt.

498 The scan spectra of C_{1s} of the native cellulose and the phosphorylated cellulose are
499 presented in Figure S4c and d. The spectra are decomposed in 4 peaks characteristics of the
500 cellulose, namely, C1(C-C), C2 (C-O), C3 (C=O) and C4 (O-C-O) at respectively, 285.0,
501 286.6, 287.8, 289.2 eV. The two spectra present high differences especially regarding the C1
502 and C2 peaks. Indeed, the grafting of phosphate groups can change the chemical environment
503 of the carbon and thus increases the C-C peak while decreasing the C-O peak (Božič et al.,
504 2014). The intensity of C-C peak increases and this can be due to the presence of phosphate
505 groups covering all of the outer surface of fibers (Ghanadpour et al., 2015; Li, Wang, Liu,
506 Xiong, & Liu, 2012).

507 The relative surface concentration of C, O and P atoms were calculated by integrating the
508 peaks of each element and results are presented in Table S1. Unfortunately after
509 phosphorylation the O/C ratio does not increase whereas a lot of oxygen is supposed to be
510 added on the cellulose with the phosphorus grafting. Indeed, one free hydroxyl groups of the
511 pristine cellulose is substituted by two new hydroxyl groups and one phosphoryl group (Božič
512 et al., 2014; Granja et al., 2001).

513 Regarding the O_{1s} scan of phosphorylated cellulose, in Figure S4f, a very small asymmetry
514 is detected and the peak can be decomposed in two peaks: 532.7 eV for O1(C-O) and 531.5
515 eV for O2 (P-O) which confirms once again the phosphorylation (Bourbigot et al., 1994). The

516 DS of the phosphate groups on the cellulose fibers is estimated as follow according to Li et
517 al.(Li et al., 2012). The obtained value is reported in Table S1.

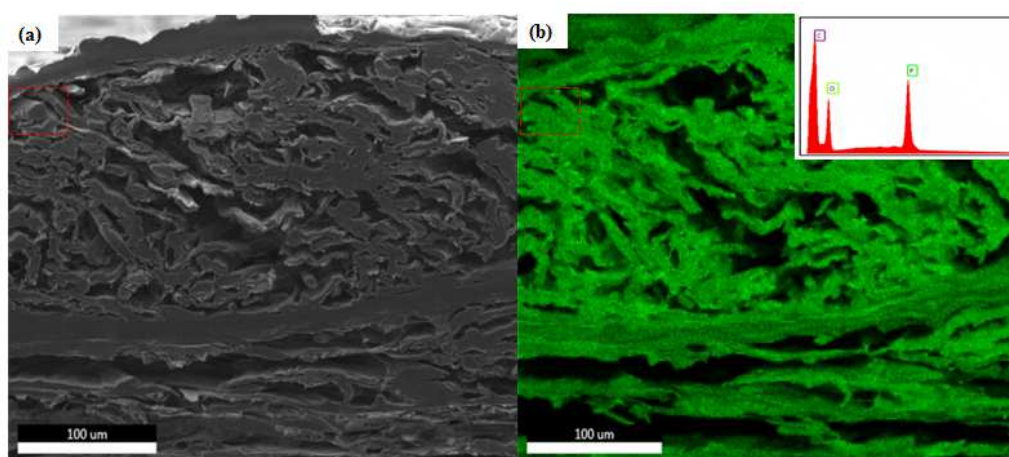
518
$$DS = \frac{O2}{O1 + O2}$$

519 The tested phosphorylated pulp presents a charge content of 2.10 mmol/g which
520 corresponds to a DS of 0.32. Here, the obtained DS is three times lower as reported in Table
521 S1. Indeed, XPS measured the surface grafting whereas the titration measure the bulk
522 grafting. The difference can be explained by different points: (i) some phosphorus can be
523 embedded in the fibers network and unseen by XPS, however, we considered that fibers are
524 well washed, (ii) the fibers washing is more efficient in surface than in the inner structure of
525 the cellulose which results in lower grafting, (iii) the grafting is heterogeneous and the
526 analysis was done on a poorly grafted part of the fibers surface.

527 To conclude, phosphorus was detected by XPS analysis but no information on the
528 phosphorylated cellulose structure is obtained using this technique.

529 3.4.5 SEM EDX

530 The phosphate group position on the fiber was then evaluated using SEM-EDX on a
531 sectional view of phosphorylated cellulose paper with a charge content of 2.1 mmol/g as
532 reported in Figure 8. Phosphorus is present in huge quantity and covered entirely the sample.
533 Even if the image scale is important compared to the fiber diameters some fibers are visible in
534 sectional view and framed in red. It seems that phosphate groups penetrate the fiber diameter
535 and are homogeneously distributed.



536 **Figure 8:** Evaluation of phosphorus position on the cellulose fibers (2.93 mmol/g) using EDX
537 images with (a) MEB images and (b) coloration of phosphorus group in green

538 3.5 Influence of the phosphorylation step on cellulose fibers

539 Fiber degradation traditionally occurs during cellulose chemical pretreatment. Cellulose
540 degradation due to the phosphorylation is evaluated measuring the degree of polymerization
541 and the crystallinity index as reported in Figure S5.

542 Partial swelling of fibers was observed when the charge content increased as well as a small
543 decrease in the crystallinity index (CI). Cellulose phosphorylation induces a fiber swelling
544 which can lead to some dissolution. A ballooning effect is visible for the sample containing
545 2.9 mmol/g of phosphate group but fibers morphologies are still maintained.

546 However, despite the high charge content of 2.9 mmol/g, cellulose I form was maintained
547 and suitable CI was obtained. Noguchi et al.(Noguchi et al., 2017) reported no crystallinity
548 change when the charge content varied from 0 to 2.2 mmol/g. Increasing the charge content
549 will drastically improve the nanofibrillation step without affecting too much the cellulose
550 fibers structure and morphology. This is confirmed by the absence of modification of the
551 carbon spectra in NMR analysis.

552 The degree of polymerization (DP) of the phosphorylated cellulose pulp with a charge
553 content of 2.1 mmol/g was measured. The phosphorylated pulp presents a DP of 628 ± 5
554 whereas the refined cellulose pulp presents a DP of 1,200. Phosphorylation as other chemical
555 pretreatments used to weaken cellulose fibers, decreases the DP of the fibers. Rol et al.(Rol et
556 al., 2017) reported a DP decrease of 50 and 75% for respectively enzymatic pretreatment and
557 TEMPO-oxidation of cellulose fiber. As observed in Figure S5 phosphorylation can lead to
558 fiber partial swelling which can result in some dissolution and thus induce a DP decrease.
559 Plus, during the phosphorylation, acid can be released and lead to DP decrease.

560 To conclude, phosphorylation leads to some fiber DP decreases and can lead to some fibers
561 swelling which will further help the nanofibrillation but preserves the cellulose crystalline
562 structure.

563 **4 Conclusion**

564 The phosphorylation of cellulose fibers was studied and optimized to increase the final
565 charge content. Different phosphate salts were tested and no effect of the Ks was reported
566 whereas the presence of ammonium counterion improves the modification rate. A poor
567 adsorption of phosphate ions on the cellulose fibers was reported and the filtration step should
568 be eliminated to strongly increase the charge content. However, the grafting should be limited
569 to avoid fiber dissolution. The grafted molecule position in the cellulose fibers and the
570 chemical structure of the phosphorylated fibers were investigated using several high level

571 techniques such as NMR, XPS, ToF-SIMS or SEM EDX. NMR analysis confirms that the
572 phosphorylation impacted all the protons network of the cellulose and that the reaction mainly
573 occurs in amorphous area of the cellulose fibers. Finally, it seems that phosphate groups do
574 not affect significantly the physical properties of cellulose fibers.

575 **Acknowledgment**

576 This research was supported by Institut Carnot Polynat (Grant agreement n° ANR-16-CARN-
577 0025-01), Centre Technique du Papier (Grenoble, France) and LabEx Tec 21 (Grant
578 agreement n° ANR-11-LABX-0030). LGP2 is part of the LabEx Tec 21 (Investissements
579 d’Avenir) and Institut Carnot Polynat.

580 **References**

- 581 Aoki, D., & Nishio, Y. (2010). Phosphorylated cellulose propionate derivatives as
582 thermoplastic flame resistant/retardant materials: influence of regioselective
583 phosphorylation on their thermal degradation behaviour. *Cellulose*, *17*(5), 963–976.
584 <https://doi.org/10.1007/s10570-010-9440-8>
- 585 Atalla, R. H., & Vanderhart, D. L. (1984). Native cellulose: a composite of two distinct
586 crystalline forms. *Science (New York, N.Y.)*, *223*(4633), 283–285.
587 <https://doi.org/10.1126/science.223.4633.283>
- 588 Atalla, R. H., & VanderHart, D. L. (1999). The role of solid state ¹³C NMR spectroscopy in
589 studies of the nature of native celluloses. *Solid State Nuclear Magnetic Resonance*,
590 *15*(1), 1–19. [https://doi.org/10.1016/S0926-2040\(99\)00042-9](https://doi.org/10.1016/S0926-2040(99)00042-9)
- 591 Bardet, R., Bras, J., Belgacem, N., Agut, P., & Dumas, J. (2014). *Patent No. WO 2014118466*
592 *(A1)*.
- 593 Bourbigot, S., Le Bras, M., Gengembre, L., & Delobel, R. (1994). XPS study of an
594 intumescent coating application to the ammonium polyphosphate/pentaerythritol fire-
595 retardant system. *Applied Surface Science*, *81*(3), 299–307.
596 [https://doi.org/10.1016/0169-4332\(94\)90287-9](https://doi.org/10.1016/0169-4332(94)90287-9)
- 597 Božič, M., Liu, P., Mathew, A. P., & Kokol, V. (2014). Enzymatic phosphorylation of
598 cellulose nanofibers to new highly-ions adsorbing, flame-retardant and
599 hydroxyapatite-growth induced natural nanoparticles. *Cellulose*, *21*(4), 2713–2726.
600 <https://doi.org/10.1007/s10570-014-0281-8>
- 601 Brodin, F. W., Gregersen, O. W. & Syverud, K. (2014). Cellulose nanofibrils: Challenges and
602 possibilities as a paper additive or coating material: A review. *Nordic Pulp and Paper*
603 *Research Journal*, *29*(01), 156–166. <https://doi.org/10.3183/NPPRJ-2014-29-01-p156-166>
- 604 Chaker, A., & Boufi, S. (2015). Cationic nanofibrillar cellulose with high antibacterial
605 properties. *Carbohydrate Polymers*, *131*, 224–232.
606 <https://doi.org/10.1016/j.carbpol.2015.06.003>

607 Coleman, R. J., Lawrie, G., Lambert, L. K., Whittaker, M., Jack, K. S., & Grøndahl, L.
608 (2011). Phosphorylation of alginate: synthesis, characterization, and evaluation of in
609 vitro mineralization capacity. *Biomacromolecules*, *12*(4), 889–897.
610 <https://doi.org/10.1021/bm1011773>

611 Davis, F. V., Findlay, J., & Rogers, E. (1949). 52—the Urea-Phosphoric Acid Method of
612 Flameproofing Textiles. *Journal of the Textile Institute Transactions*, *40*(12), T839–
613 T854. <https://doi.org/10.1080/19447024908660067>

614 Dufresne, A. (2013). Nanocellulose: a new ageless bionanomaterial. *Materials Today*, *16*(6),
615 220–227. <https://doi.org/10.1016/j.mattod.2013.06.004>

616 Gallagher, D. M. (1965). *Phosphorylation of cotton with inorganic phosphates*. Retrieved
617 from <https://patents.google.com/patent/US3488140A/en>

618 Ghanadpour, M., Carosio, F., Larsson, P. T., & Wågberg, L. (2015). Phosphorylated
619 Cellulose Nanofibrils: A Renewable Nanomaterial for the Preparation of Intrinsically
620 Flame-Retardant Materials. *Biomacromolecules*, *16*(10), 3399–3410.
621 <https://doi.org/10.1021/acs.biomac.5b01117>

622 Granja, P. L., Pouységu, L., Pétraud, M., De Jéso, B., Baquey, C., & Barbosa, M. A. (2001).
623 Cellulose phosphates as biomaterials. I. Synthesis and characterization of highly
624 phosphorylated cellulose gels. *Journal of Applied Polymer Science*, *82*(13), 3341–
625 3353. <https://doi.org/10.1002/app.2193>

626 Ichikawa, S., Wada, S., Masuda, S., & Hasegawa, T. (1979). *Patent No. JP54138060A*.

627 Inagaki, N., Nakamura, S., Asai, H., & Katsuura, K. (1976). Phosphorylation of cellulose with
628 phosphorous acid and thermal degradation of the product. *Journal of Applied Polymer
629 Science*, *20*(10), 2829–2836. <https://doi.org/10.1002/app.1976.070201017>

630 Isogai, A., Saito, T., & Fukuzumi, H. (2011). TEMPO-oxidized cellulose nanofibers.
631 *Nanoscale*, *3*(1), 71–85. <https://doi.org/10.1039/C0NR00583E>

632 Katsuura, K., & Mizuno, H. (1966). Flameproofing of cotton fabrics with urea and phosphoric
633 acid in organic solvent. *Sen'i Gakkaishi*, *22*(11), 510–514.
634 <https://doi.org/10.2115/fiber.22.510>

635 Klemm, D., Kramer, F., Moritz, S., Lindström, T., Ankerfors, M., Gray, D., & Dorris, A.
636 (2011). Nanocelluloses: A New Family of Nature-Based Materials. *Angewandte
637 Chemie International Edition*, *50*(24), 5438–5466.
638 <https://doi.org/10.1002/anie.201001273>

639 Kokol, V., Božič, M., Vogrinčič, R., & Mathew, A. P. (2015). Characterisation and properties
640 of homo- and heterogenously phosphorylated nanocellulose. *Carbohydrate Polymers*,
641 *125*, 301–313. <https://doi.org/10.1016/j.carbpol.2015.02.056>

642 Lagier, C. M., Zuriaga, M., Monti, G., & Olivieri, A. C. (1996). Urea-phosphoric acid
643 complex studied by variable temperature ³¹P NMR spectroscopy and semiempirical
644 calculations. *Journal of Physics and Chemistry of Solids*, *57*(9), 1183–1190.
645 [https://doi.org/10.1016/0022-3697\(95\)00294-4](https://doi.org/10.1016/0022-3697(95)00294-4)

646 Lavoine, N., Desloges, I., Dufresne, A., & Bras, J. (2012). Microfibrillated cellulose – Its
647 barrier properties and applications in cellulosic materials: A review. *Carbohydrate
648 Polymers*, *90*(2), 735–764. <https://doi.org/10.1016/j.carbpol.2012.05.026>

649 Li, K., Wang, J., Liu, X., Xiong, X., & Liu, H. (2012). Biomimetic growth of hydroxyapatite
650 on phosphorylated electrospun cellulose nanofibers. *Carbohydrate Polymers*, *90*(4),
651 1573–1581. <https://doi.org/10.1016/j.carbpol.2012.07.033>

652 Lim, S., & Seib, P. A. (1993). Preparation and pasting properties of wheat and corn starch
653 phosphates. *Cereal Chemistry*. Retrieved from [http://agris.fao.org/agris-](http://agris.fao.org/agris-search/search.do?recordID=US19940103186)
654 [search/search.do?recordID=US19940103186](http://agris.fao.org/agris-search/search.do?recordID=US19940103186)

655 Littunen, K., Snoei de Castro, J., Samoylenko, A., Xu, Q., Quaggin, S., Vainio, S., & Seppälä,
656 J. (2016). Synthesis of cationized nanofibrillated cellulose and its antimicrobial
657 properties. *European Polymer Journal*, *75*, 116–124.
658 <https://doi.org/10.1016/j.eurpolymj.2015.12.008>

659 Manet, S. (2007). *Effet de contre-ion sur les propriétés d'amphiphiles cationiques* (Phdthesis,
660 Université Sciences et Technologies - Bordeaux I). Retrieved from [https://tel.archives-](https://tel.archives-ouvertes.fr/tel-00250098/document)
661 [ouvertes.fr/tel-00250098/document](https://tel.archives-ouvertes.fr/tel-00250098/document)

662 Montanari, S., Roumani, M., Heux, L., & Vignon, M. R. (2005). Topochemistry of
663 Carboxylated Cellulose Nanocrystals Resulting from TEMPO-Mediated Oxidation.
664 *Macromolecules*, *38*(5), 1665–1671. <https://doi.org/10.1021/ma048396c>

665 Mucalo, M. R., Kato, K., & Yokogawa, Y. (2009). Phosphorylated, cellulose-based substrates
666 as potential adsorbents for bone morphogenetic proteins in biomedical applications: A
667 protein adsorption screening study using cytochrome C as a bone morphogenetic
668 protein mimic. *Colloids and Surfaces B: Biointerfaces*, *71*(1), 52–58.
669 <https://doi.org/10.1016/j.colsurfb.2009.01.004>

670 Naderi, A., Lindström, T., Weise, C. F., Flodberg, G., Sundström, J., Junel, K., ... Runebjörk,
671 A. M. (2016). Phosphorylated nanofibrillated cellulose: production and properties.
672 *Nordic Pulp and Paper Research Journal*, *31*(01), 020–029.
673 <https://doi.org/10.3183/NPPRJ-2016-31-01-p020-029>

674 Noguchi, Y., Homma, I., & Matsubara, Y. (2017). Complete nanofibrillation of cellulose
675 prepared by phosphorylation. *Cellulose*, *24*(3), 1295–1305.
676 <https://doi.org/10.1007/s10570-017-1191-3>

677 Nuessle, A. C., Ford, F. M., Hall, W. P., & Lippert, A. L. (1956). Some Aspects of the
678 Cellulose-Phosphate-Urea Reaction. *Textile Research Journal*, *26*(1), 32–39.
679 <https://doi.org/10.1177/004051755602600105>

680 Ott, E., Spurlin, H. M., Grafflin, M. W., Bikales, N. M., & Segal, L. (1954). *Cellulose and*
681 *cellulose derivatives*. Interscience Publishers.

682 Pasqui, D., Rossi, A., Di Cintio, F., & Barbucci, R. (2007). Functionalized Titanium Oxide
683 Surfaces with Phosphated Carboxymethyl Cellulose: Characterization and Bonelike
684 Cell Behavior. *Biomacromolecules*, *8*(12), 3965–3972.
685 <https://doi.org/10.1021/bm701033u>

686 Petreus, T., Stoica, B. A., Petreus, O., Goriuc, A., Cotrutz, C.-E., Antoniac, I.-V., & Barbu-
687 Tudoran, L. (2014). Preparation and cytocompatibility evaluation for hydrosoluble
688 phosphorous acid-derivatized cellulose as tissue engineering scaffold material. *Journal*
689 *of Materials Science: Materials in Medicine*, *25*(4), 1115–1127.
690 <https://doi.org/10.1007/s10856-014-5146-z>

691 Reid, J. D., & Mazzeno, L. W. (1949). Preparation and Properties of Cellulose Phosphates.
692 *Industrial & Engineering Chemistry*, 41(12), 2828–2831.
693 <https://doi.org/10.1021/ie50480a039>

694 Reid, J. D., Mazzeno, L. W., & Buras, E. M. (1949). Composition of Two Types of Cellulose
695 Phosphates. *Industrial & Engineering Chemistry*, 41(12), 2831–2834.
696 <https://doi.org/10.1021/ie50480a040>

697 Rol, F., Belgacem, M. N., Gandini, A., & Bras, J. (2018). Recent advances in surface-
698 modified cellulose nanofibrils. *Progress in Polymer Science*.
699 <https://doi.org/10.1016/j.progpolymsci.2018.09.002>

700 Rol, F., Karakashov, B., Nechyporchuk, O., Terrien, M., Meyer, V., Dufresne, A., ... Bras, J.
701 (2017). Pilot scale twin screw extrusion and chemical pretreatment as an energy
702 efficient method for the production of nanofibrillated cellulose at high solid content.
703 *ACS Sustainable Chemistry & Engineering*.
704 <https://doi.org/10.1021/acssuschemeng.7b00630>

705 Saini, S., Yücel Falco, Ç., Belgacem, M. N., & Bras, J. (2016). Surface cationized cellulose
706 nanofibrils for the production of contact active antimicrobial surfaces. *Carbohydrate*
707 *Polymers*, 135, 239–247. <https://doi.org/10.1016/j.carbpol.2015.09.002>

708 Suflet, D. M., Chitanu, G. C., & Popa, V. I. (2006). Phosphorylation of polysaccharides: New
709 results on synthesis and characterisation of phosphorylated cellulose. *Reactive and*
710 *Functional Polymers*, 66(11), 1240–1249.
711 <https://doi.org/10.1016/j.reactfunctpolym.2006.03.006>

712 Yajima, S. (2018, August 29). *Announcement regarding expanding lineup of phosphorylated*
713 *CNF slurry samples*. Retrieved from
714 [https://www.ojiholdings.co.jp/Portals/0/resources/content/files/english/ir/news/2018/
715 WCd2Wuj.pdf](https://www.ojiholdings.co.jp/Portals/0/resources/content/files/english/ir/news/2018/WCd2Wuj.pdf)

716 Yurkshtovich, N. K., Yurkshtovich, T. L., Kaputskii, F. N., Golub, N. V., & Kosterova, R. I.
717 (2007). Esterification of viscose fibres with orthophosphoric acid and study of their
718 physicochemical and mechanical properties. *Fibre Chemistry*, 39(1), 31–36.
719 <https://doi.org/10.1007/s10692-007-0007-x>

720